Interlibrary Loans and Journal Article Requests

Notice Warning Concerning Copyright Restrictions:

The copyright law of the United States (Title 17, United States Code) governs the making of photocopies or other reproductions of copyrighted materials.

Under certain conditions specified in the law, libraries and archives are authorized to furnish a photocopy or other reproduction. One specified condition is that the photocopy or reproduction is not to be *"used for any purpose other than private study, scholarship, or research."* If a user makes a request for, or later uses, a photocopy or reproduction for purposes in excess of "fair use," that user may be liable for copyright infringement.

Upon receipt of this reproduction of the publication you have requested, you understand that the publication may be protected by copyright law. You also understand that you are expected to comply with copyright law and to limit your use to one for private study, scholarship, or research and not to systematically reproduce or in any way make available multiple copies of the publication.

The Stephen B. Thacker CDC Library reserves the right to refuse to accept a copying order if, in its judgment, fulfillment of the order would involve violation of copyright law.

Terms and Conditions for items sent by e-mail:

The contents of the attached document may be protected by copyright law. The CDC copyright policy outlines the responsibilities and guidance related to the reproduction of copyrighted materials at CDC. If the document is protected by copyright law, the following restrictions apply:

- You may print only one paper copy, from which you may not make further copies, except as maybe allowed by law.
- You may not make further electronic copies or convert the file into any other format.
- You may not cut and paste or otherwise alter the text.

Bulletin of the Seismological Society of America, Vol. 92, No. 8, pp. 3321–3328, December 2002

Comparison of Body-Wave Displacement with Damage Observations of a Rockburst, Coeur d'Alene Mining District, Idaho

by Kenneth F. Sprenke, Brian G. White, Alan C. Rohay, Jeffrey K. Whyatt, and Michael C. Stickney

Abstract Fault-plane solutions for seismic events in the deep underground mines of the Coeur d'Alene Mining District in northern Idaho have been difficult to reconcile with actual observations of mine damage. Examination of rockburst damage in stopes as well as measurements of slip movements on bedding planes suggests that rockbursts in the Lucky Friday Mine are closely associated with gradual bedding-plane slip. This progressive slip reduces the physical dimensions of stopes and increases compressive stress resulting in sudden implosive failure of the stope margins. Thus, much of the difficulty in evaluating seismological data arises from the implosional nature of these rockbursts, making the first motion of the events difficult to interpret. In the summer of 1998, we acquired several months of high-quality seismic data from five stations in the vicinity of the Lucky Friday Mine. This is the first time that a network of high dynamic-range, three-component instruments has been deployed in this mining district. On 29 August, 1988 at 6:09 UTC, a M_L 2.9 event occurred at the Lucky Friday Mine. This event resulted from bedding-plane slip and caused extensive damage in the mine that was carefully documented. Using a least-squares procedure, we were able to find a well-constrained moment tensor solution that matches the *P* and *S* displacement amplitudes measured at the five temporary stations. We derived a model of the mechanism to compare with the underground observations of bedding-plane slip and damage. We conclude that high-quality seismological instrumentation is required if meaningful results are to be obtained for understanding the source mechanisms of shear-implosional rockbursts.

Introduction

The Lucky Friday Mine in northern Idaho is among the most seismically active in North America (e.g., Blake and Cuvelier, 1990; Jenkins *et al.*, 1990; Sprenke *et al.*, 1991; Scott, 1993, Whyatt *et al.*, 1993; Friedel *et al.*, 1995; White and Whyatt, 19990a). Reconciling seismic fault-plane solutions and rockburst damage has long been an issue at this mine (Jung *et al.*, 1995; Whyatt *et al.*, 1997; Talebi, 1997). In this article, we report on a relatively large seismic event (M_L 2.9) in the Lucky Friday Mine that occurred at 6:09 29 August, 1998 UTC (9:09 pm 28 August PDT). What makes this particular event unique among the many M_L 3 events that occur annually in this mining district is that the bedding-plane slip associated with the event was visible, in-mine damage was well-documented, and five temporary high-quality high-dynamic range accelerometers within 5 km of the mine recorded the event. The bedding slip and damage observations bring independent objective data to aid in the interpretation of the seismic mechanism.

At the Lucky Friday Mine, rockbursts in stopes are commonly associated with progressive bedding slip. The moderately dipping metasedimentary strata have a tendency to slip along their bedding planes into the stopes located along the nearly vertical vein. This results in the axis of principal maximum stress directed parallel to the dip of the bedding. How the stope might fail under this condition depends on the location of the slip plane relative to the stope and the geometry of the mining-induced fractures surrounding the stope (White and Whyatt, 1999b).

The event described here resulted in extensive damage in the 05 stope 1750 m underground (Fig. 1). Rock was expelled from the sidewalls, and the overhead cemented sandfill failed along the length of the stope. Bedding slip associated with this event was definitively documented, by offsets of at least 15 cm in marks, previously painted across exposed argillite interbeds, some 30 m north of the 05 stope in the access ramp (Fig. 1). In this access ramp, the bedding dips 35°–45° south, so the observed slip plane is stratigraphically about 20 m below the 05 stope. Bedding slip may have occurred closer to the stope as well, but all other reference points were disturbed by the event. Although this bedding

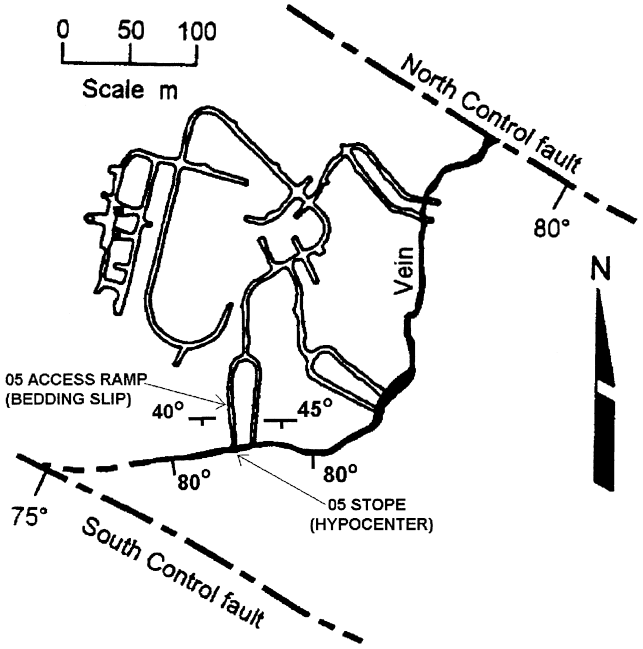

Figure 1. Plan view of the of the Lucky Friday Mine some 1750 m below the surface. The general location of the hypocenter is shown as is the location of the documented bedding slip associated with the event. Note that the bedding dips moderately south, intersecting the steeply dipping vein, promoting slip along bedding planes as the vein is mined.

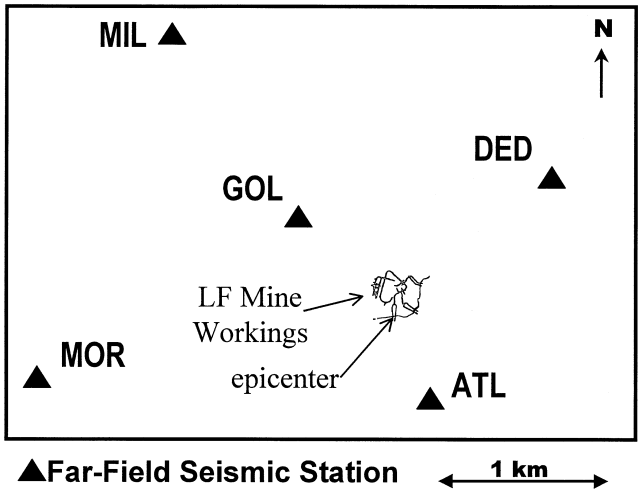

Figure 2. Locations of the five temporary accelerometer stations with respect to the mine workings and the epicenter.

slip is thought to have possibly occurred during the seismic event, more gradual progressive aseismic fault slip has been documented over a period of six weeks in nearby access ramps. Damage to the stope in this event included apparent compression of the sidewalls and overlying sandfill to failure.

Moment Tensor Inversion

To study the seismic mechanism, we performed a moment tensor inversion in the time domain using the displacement amplitudes of body-wave phases derived from five strong-motion accelerometers deployed in the immediate area of the mine (Fig. 2). The five stations were located at a variety of azimuths, inclinations, and slant distances with respect to the hypocenter (Table 1). One station (ATL) was located in a shallow adit about 50 m below the ground surface; the other four accelerometers were on the surface. Thus all stations were well above the hypocenter that occurred 1750 m deep in the mine. An underground geophone array operated within the mine by Hecla Mining Company provided a hypocenter location, probably accurate to about 30 m, placing the burst in the general vicinity of the 05 stope, although its specific location relative to the 3-m-wide stope is not known.

The polarities and amplitudes of the integrated acceleration at MOR were checked against a colocated broadband Guralp CMG-3 broadband seismometer; peak or root mean square (rms) amplitudes always agree within 8% after filtering both below 1 Hz. At the other stations, the calibrations were checked using internal calibration pulses in the field, and polarities were checked for signals from two more distant events located at the Galena mine (12 km west of the westernmost station MOR). Unfortunately, ATL did not record these events, so polarities were confirmed from amplitude and polarity for events from several different parts of the Lucky Friday Mine.

Measurement of displacement from accelerometer records is difficult because the accelerometer records must be integrated twice. Although the instrument response is flat to low frequency for these instruments, instrument noise increases and is amplified on integration. A four-pole butterworth high-pass filter was applied at 0.5 Hz to the de-meaned and end-tapered accelerograms before each of the two integration steps. Comparison of the spectra indicate that frequencies above 1 Hz are little affected, and although a lower frequency limit would be desirable, it becomes difficult to measure amplitudes at the dominant high frequency with the residual low-frequency components not completely removed. The corner frequency of the largest event studied here was over 10 Hz, and this leaves much of the signal relatively free from the effects of the filtering. Considering that we digitized at 200 Hz, the digital brick-wall filters have no significant effect on signals below 80 Hz.

The low resultant amplitudes on the transverse components of the *P* phase after rotation of the horizontal components (Fig. 3) suggest that the source to station azimuths are not a major source of error. Inspection of the displacement records shows reasonably simple displacement pulses at most stations with the notable exception of DED, which shows an extended coda. The quality of the records varies from excellent to poor. At MIL, for example, the station is

Table 1
Network Focal Plane Coverage

Station	Azimuth from Source (°)	Hypocentral Distance (m)	Inclination to Source (°)	*P* Emergence Angle (°)	*S* Emergence Angle (°)	*P* Takeoff Angle (°)	*S* Takeoff Angle (°)
MOR	261	2663	37	45	79	61	90
MIL	324	2948	39	51	51 (?)	63	63 (?)
DED	45	2310	55	57	73	37	53
GOL	319	1997	64	72	70	34	34
ATL	160	1766	73	78	73	22	22

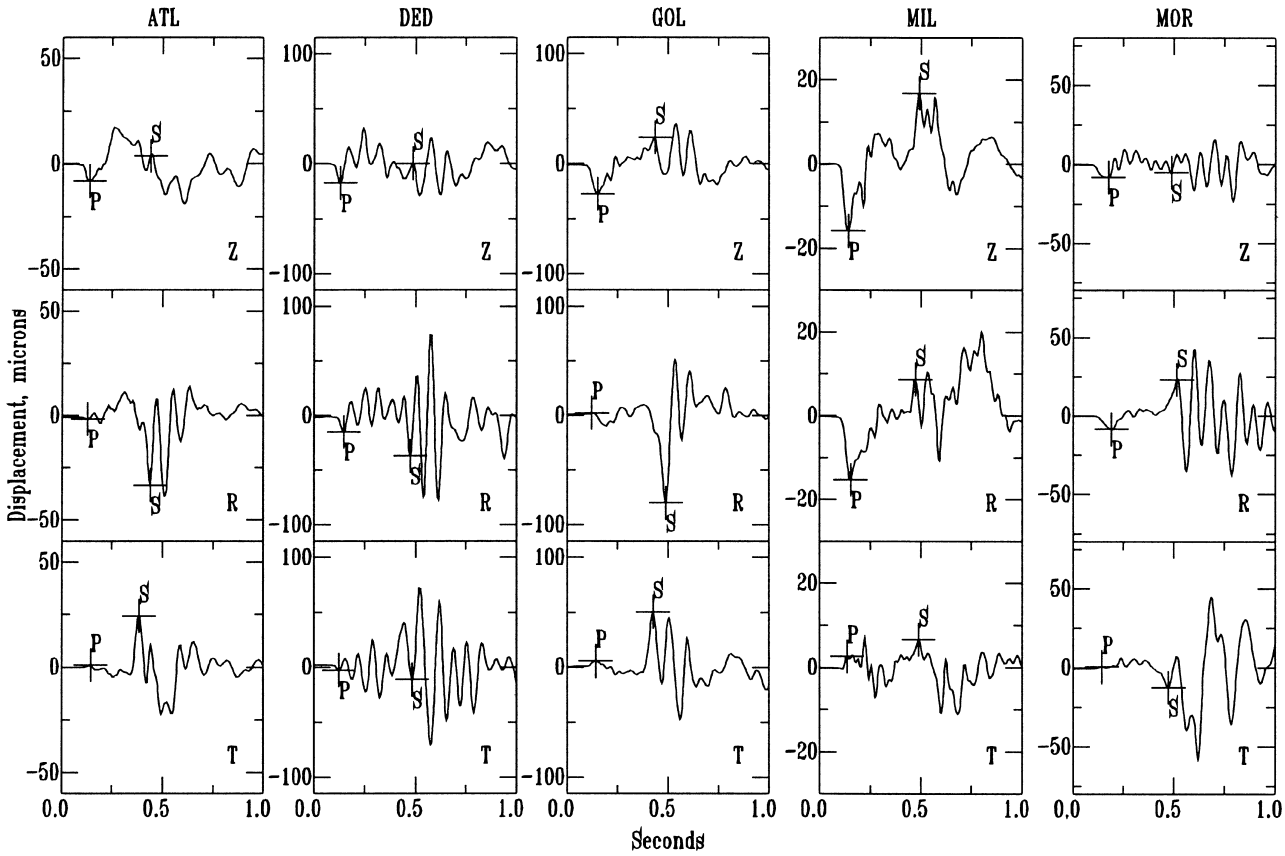

Figure 3. Displacement records for the large event after rotation of the horizontal components. Vertical (Z), radial (R), and transverse (T) components are shown.

located at the base of a very steep mountain. A reflected *P* phase from the opposite side of the mountain unfortunately interferes with the *S* phase, making the *S* arrivals on the vertical and radial components uncertain. The initial *S* phase at many of the stations is immediately followed by surface-wave trains that, in view of the extreme topographic relief of the mine area, we did not attempt to model.

Our measurements of the displacement of the initial *P* and *S* pulses were made by transforming the three-component records were into a ray-path spherical-coordinate system with the source at the origin to make the *P*, *SV*, and *SH* phases distinctly identifiable on the r, θ, and ϕ components, respectively. The results, as illustrated for station MOR in Figure 4, are far from ideal, but the initial *P*, *SV*, and *SH* pulses are evident. An anisotropy of about 4% appears to be present in the mine area, the initial *SH* pulse arriving slightly ahead of the *SV* pulse.

Following the recommendation of Trifu *et al.* (2000), we employed only the excellent picks in the inversion process. The *SV* picks at MIL were discarded for the reason stated above. The *SV* picks at DED, and ATL as well as the *SH* pick at DED were also discarded in the moment tensor analysis because of polarity uncertainty. However, our initial estimates at these picks nonetheless were found consistent in polarity with the final moment tensor solution.

Using free surface equations (e.g., Udias, 1999, equation 5.132), the actual angles of emergence were calculated along with the displacement amplitudes of the incident *P*,

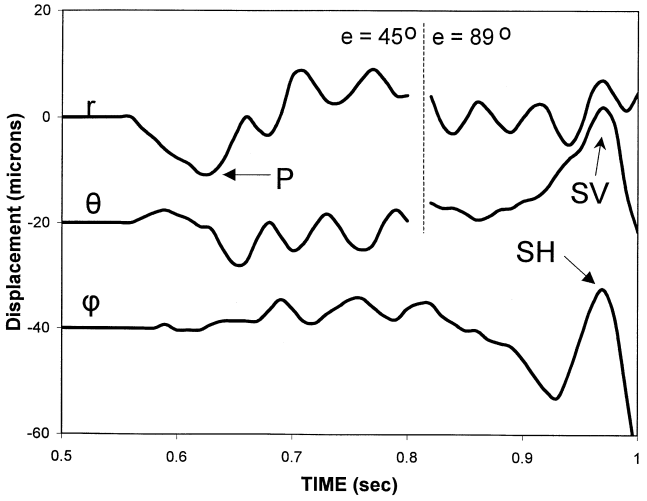

Figure 4. Body-wave displacements at station MOR transformed to the ray-path coordinate system. The angles of emergence (e) were found to be different for the *P* and *S* phases, thus the break in the traces. The lower two traces are offset 20 and 40 microns, respectively.

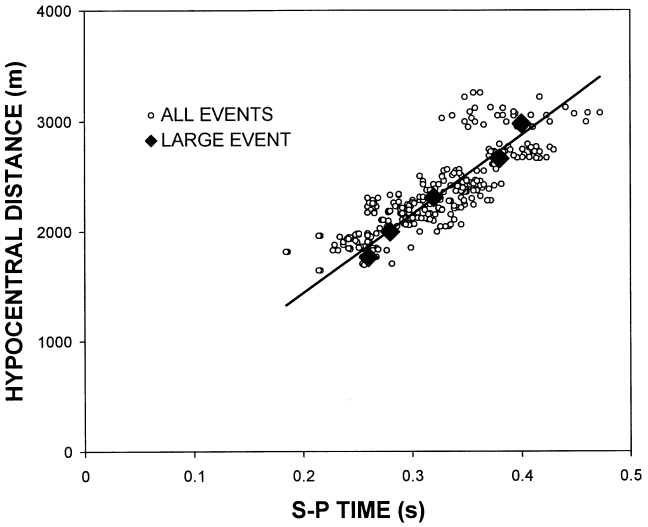

Figure 5. *S-P* times measured from events located in the mine as recorded by the temporary accelerometer network. The best-fit line shown through all measurements has a slope of 7198 ± 34 m/sec. In a Poisson solid, this result translates to a *P* velocity of 5.25 ± 0.02 km/sec.

SV, and *SH* (Table 1). We note that the actual angles of emergence are all greater than the inclination angle predicted from the straight-line path from source to receiver. To compensate, we assume a linear increase in velocity with depth, slightly circular wavepaths, and takeoff angles from the source as shown in Table 1. We have no geological evidence to substantiate a more sophisticated velocity model, but this assumption seems better than an isotropic and homogeneous velocity model that is inconsistent with our observed emergence angles.

In order to compare observed and modeled displacement amplitudes on a stereonet, the observations were reduced to a unit sphere of radius 1 km surrounding the hypocenter. This correction for geometric spreading was accomplished by multiplying the observed displacements, after correction for the free surface effect and anelastic attenuation, by the seismic path distance in km to each station.

We did not have accurate relative timing between our stations and the in-mine geophone system. However, our evaluation of *S-P* times from this event and many smaller events in the mine (Fig. 5) suggests a *P*-wave velocity of 5.25 km/sec at the source. Previous in-mine tomographic studies suggested a source velocity of 4.78 km/sec (Friedel *et al.*, 1995). A district-wide study found 5.74 km/sec (Stickney and Sprenke, 1993). Thus we used 5.25 ± 0.50 km/sec for the *P*-wave velocity in our analysis. For the metasedimentary rocks in the mine area, we used a density of 2.7, a Poisson's ratio of 0.25, and quality factors (Q) of 250 for *P* and 150 for *S*. The 10% uncertainty in velocity translates to about a 30% uncertainty in displacement calculations. The range of reasonable Q values results in no more than about a 10% uncertainty in the displacement calculations. The possible error from scattering is probably as large as the uncertainty associated with the anelastic attenuation. Combining these uncertainties, assuming they are independent, results in a 33% uncertainty in the displacements. Although this uncertainty seems large, work by Trifu *et al.* (2000) suggested that meaningful moment tensor inversions can be obtained even with such noisy data, provided that the *S*-wave polarities are correct.

Following the method for moment tensor inversion of mining-related events by McGarr (1992), the moment tensor of the seismic event was estimated from amplitude measurements of *P*, *SV*, and *SH* body-wave phases in the far field by linearly inverting:

$$A_{ij}m_j = u_i, \tag{1}$$

where u_i consists of the i sampled observations of ground displacement of body-wave phases at the various stations and $m_j = [M11, M12, M22, M13, M23, M33]$, a vector containing the six moment tensor elements to be determined (e.g., Gibowicz and Kijko, 1994). To estimate the matrix A_{ij}, we used the body-wave pulse amplitudes measured from synthetic seismograms, generated using unit values of the moment tensor elements at ray-path geometries appropriate for the observations. For each observation i, six synthetic seismograms were calculated, one for each element j of the moment tensor. For the first synthetic seismogram, $M11 = 1$, and all other elements are set to zero; for the second synthetic seismogram, $M22 = 1$, and all other elements are zero; and so forth for each element of the moment tensor. The synthetic seismograms are calculated on a unit sphere of radius 1 km for the azimuth and takeoff angle appropriate for each of the i observations. From each of the $i \times j$ (66 in

our case) synthetic seismograms, we measured the maximum displacement of the body-wave pulse in question for comparison with our 11 observations of the same. Thus, the A_{ij} matrix components are the measurements from the synthetic seismograms, for each m_j, corresponding to the actual ground-motion records of displacement (after correction for the free surface and reduction to the unit sphere). The synthetic seismograms were computed assuming that the components of the moment tensor have same moment rate function, defined as follows:

$$M_0'(t) = M_0 f(1 - \cos 2\pi ft) \quad \text{for } 0 \le t \le 1/f, \qquad (2)$$
$$M_0'(t) = 0 \text{ otherwise,}$$

where M_0 is the scalar moment, t is time, and f is the inverse of the displacement pulse duration (McGarr, 1992). Based on inspection of the displacement records, we used $f \approx 10$ Hz.

To estimate the moment tensor elements, we then solved the overdetermined set of equations (1) to find the best fit in a least-squares sense of the six independent moment tensor elements to our 11 observed displacement amplitudes. We used equation (10) from Stump and Johnson (1977) to estimate the standard errors of the estimates given the 33% uncertainty in our data.

Results

The displacement amplitudes predicted by the best-fit moment tensor solution are displayed on the upper hemisphere of equal area stereonets in Figure 6 along with the reduced observations. A scatter diagram of the observed and modeled displacements (Figure 7) shows a correlation coefficient (R^2) of 0.92 and no discrepant polarities. The moment tensor for the best-fit shear implosion is:

$$\mathbf{m} = [-0.56 \pm 0.07 \ -0.73 \pm 0.10 \ -0.40 \pm 0.10 \ -0.06 \pm 0.05 \ 0.22 \pm 0.04 \ -0.46 \pm 0.05] \times 10^{13} \text{ N m.} \qquad (3)$$

The standard errors are acceptably low considering the large uncertainties in our displacement amplitudes.

The negative trace of the moment tensor indicates a significant implosional component in the source. In diagonalized form:

$$\mathbf{m}(\text{diag}) = [M11 \ M22 \ M33] = [-0.63 \pm 0.07 \ -1.07 \pm 0.08 \ 0.01 \pm 0.08] \times 10^{13} \text{ N m} \qquad (4)$$

with eigenvectors representing the directions of the seismic I, P, and T axes, respectively, in an east–north–up coordinate system given by:

$$\begin{matrix} (0.92 \pm 0.04 & 0.33 \pm 0.11 & -0.20 \pm 0.10) \\ (0.15 \pm 0.11 & -0.79 \pm 0.10 & -0.60 \pm 0.10) \\ (0.35 \pm 0.10 & -0.52 \pm 0.08 & 0.78 \pm 0.07). \end{matrix} \qquad (5)$$

The I axis plunges gently (12° ± 6°) eastward, consistent with the east–west strike of the bedding and vein. The P axis plunges moderately (38° ± 7°) southward, parallel to the dip of bedding. The T axis plunges (51° ± 6°) northward, normal to the bedding planes. Thus, because we know from the documented slip in the access ramp that this event is associated with progressive bedding-plane slip, we have the interesting result that the axis of maximum extensional strain (T axis) is normal to the axis of maximum principle stress (dip angle of the bedding impinging upon the stope).

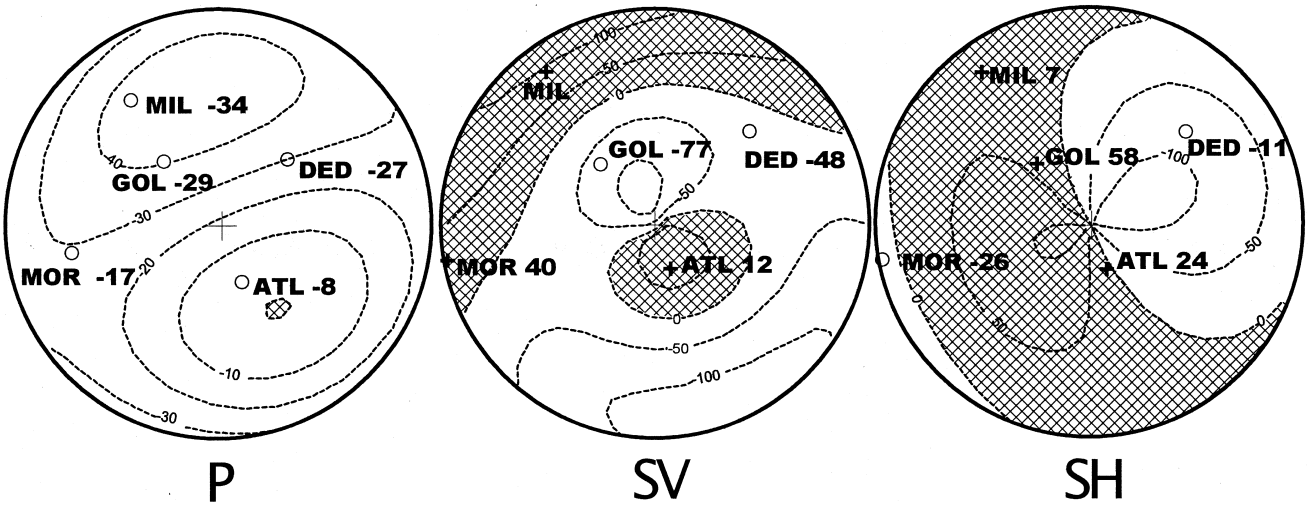

Figure 6. Contours of modeled displacements at a unit 1-km distance from the source projected onto the upper hemisphere of an equal-area stereographic projection. Also shown, for comparison, are the observed displacements (microns), after reduction to a 1 km unit distance from the source.

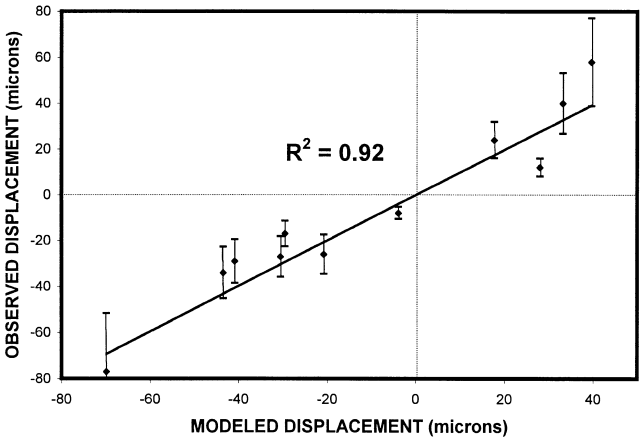

Figure 7. Regression of observed and modeled displacements.

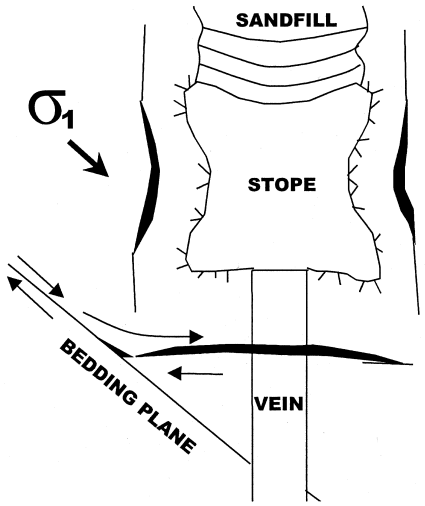

Figure 8. Cartoon showing slab formation around stopes in the Lucky Friday Mine. Mining-induced extensional fractures induced by the cavity form parallel to the sidewalls and the floor of the stope. Gradual aseismic bedding slip is accommodated by shallow thrust faulting along the preexisting horizontal extension fractures below the stope. Buckling of the upper plate of the thrust causes the sidewall slabs to buckle as well and implode into the slope. The principal axis of maximum stress ($\sigma 1$) is directed down the slipping bedding plane.

Discussion

Dipping metasedimentary beds in the Lucky Friday Mine gradually slip into stopes located along a nearly vertical vein (Fig. 8). When the slip is stratigraphically below the stope, as with the case of the 29 August event, White and Whyatt (1999b) have hypothesized that sudden seismic failure might occur in the three ways.

If the progressive slip is occasionally halted by asperities on the bedding plane, the bedding plane itself might fail violently. In this case, the seismic mechanism would be that of a double couple, generating normal slip parallel to bedding, with a near vertical axis of maximum principal strain (*P* axis). For the event under consideration, we can rule this interpretation out because no simple dip-slip fault solution of this orientation can explain the seismic polarities observed.

The second possibility is that, if the stress is concentrated at the sidewall-floor junction, thin delaminated bedding layers might buckle in a rockburst and implode diagonally upward into the opening, damaging the sidewalls. In this case, the seismic mechanism would be that of an anisotropic implosion with the axis of maximum extensional strain normal to the bedding-plane orientation. For the event under consideration, this interpretation is consistent with our seismic result in so far that the *T* axis was found normal to bedding, as well as with the observed sidewall damage. However, the form of the diagonalized moment tensor solution is inconsistent with theoretical models of anisotropic implosions (such as crack closures and mine collapses) for which $M11 = M22 = \frac{1}{3}M33$ (e.g., Aki and Richards, 1980; Taylor, 1994; Pechmann *et al.*, 1995). Thus we can rule out this interpretation as well.

In the last of the proposed models, thrust faulting along subhorizontal extensional fractures might be promoted, leading to compression and buckling of slabs surrounding the stope (Fig. 8). In this case, the seismic mechanism would be a shear implosion with a *P* axis dipping about 45° southward (parallel to bedding) and a *T* axis normal to bedding. The seismic signature of the event would be a shear implosion, combining shallow thrusting along preexisting horizontal extension fractures beneath the stope with implosion of the cavity.

To investigate this mechanism further, we decompose our diagonalized solution (4) as follows, preserving the principal axes:

$$\mathbf{m}(\text{diag}) = [M11\ M22\ M33] = \mathbf{m}(\text{imp}) + \mathbf{m}(\text{dc1}) + \mathbf{m}(\text{dc2}), \quad (6)$$

where m(imp) is the isotropic implosional component and m(dc1) and m(dc2) are major and minor double couples. We find

$$\begin{aligned} \mathbf{m}(\text{imp}) &= [-0.56\ -0.56\ -0.56] \times 10^{13}\text{N m} \\ \mathbf{m}(\text{dc1}) &= [0\ -0.57\ 0.57] \times 10^{13}\text{N m} \\ \mathbf{m}(\text{dc2}) &= [-0.06\ 0.06\ 0] \times 10^{13}\text{N m}. \end{aligned} \quad (7)$$

The net deviatoric moment is comparable in size to the implosional moment and is dominated by the major double couple. The major double couple is consistent with near horizontal thrust motion along a plane dipping very gently northward, the upper block moving southward. This result

is suggestive of thrust slip along the preexisting extension fractures below the stope.

Thus the seismic result supports the interpretation of the rockburst illustrated in Figure 8. Stress, generated by bedding-plane slip into the stope, builds up in the unmined material between the stope and the slipping bedding-plane. This rock mass eventually fails by sudden thrust offset on the horizontal extension fractures below the cavity, causing buckling and violent failure of the slabs surrounding the stope.

In the Lucky Friday Mine, mining proceeds downward to reduce rockburst hazard. This is accomplished by maximizing the vertical distance between the miners and any remnant pillars of highly stressed material that may lie along the vein above them. The 29 August event, however, was a failure in the unmined material, not above, but below the stope. Recognition of this failure mechanism thus provides critical information for the proper design of future mitigation procedures for this type of burst.

Conclusion

Reconciling seismic fault-plane solutions and rockburst damage has been problematic at the Lucky Friday Mine. Much of the confusion arises from the presence of mining-related fractures in the vicinity of openings which form planes of weakness for seismic slip and which allow the stope margins to buckle and implode violently into the openings. For the 29 August event, the deployment of state-of-the-art, high dynamic range, instrumentation made possible the reconciliation of far-field seismological information and underground observations in the mine. A shear implosional model with an axis of maximum principal extension oriented normal to bedding, explains the seismic data, the damage to the stope margins, and the observed bedding slip displacement in the access ramp. Often, because of the nature of the underground environment, direct observations of rockburst damage are confusing and difficult to interpret. Reliable information from seismic mechanisms would greatly enhance the damage assessment process.

Acknowledgments

We gratefully acknowledge the cooperation and assistance of Hecla Mining Company's Lucky Friday Mine. We especially thank Clyde Peppin, Doug Bayer, Wilson Blake, and Bill Jacobsen. This research was partially supported by NIOSH and by DSWA01-97-C-1024, U.S. Department of Defense, Defense Threat Reduction Agency.

References

Aki, A., and P. G. Richards (1980). *Quantitative Seismology: Theory and Methods*, Freeman, San Francisco.

Blake, W., and D. Cuvelier (1990). Developing reinforcement requirements for rockburst conditions at Hecla's Lucky Friday Mine, in *Proceedings of the 2nd International Symposium on Rockbursts and Seismicity in Mines 1988*, Balkema, Rotterdam, 407–409.

Friedel, M. J., M. J. Jackson, D. F. Scott, T. J. Williams, and M. S. Olson (1995). 3-D tomographic imaging of anomalous conditions in a deep silver mine, *J. Appl. Geophys.* **34,** 1–21.

Gibowicz, S. J., and A. Kijko (1994). *An Introduction to Mining Seismology*, Academic Press, San Diego, 399 pp.

Jenkins, F. M., T. J. Williams, and C. J. Wideman (1990). Analysis of four rockbursts in the Lucky Friday Mine, Mullan, Idaho, USA, *International Deep Mining Conference, 1990: Technical Challenges in Deep Level Mining: South African Institute of Mining and Metallurgy*, D. A. J. Ross-Watt and P. D. K. Robinson (Editors), 1201–1212.

Jung, S. J., P. B. Lourence, and K. F. Sprenke (1995). Fault plane solutions of mining-induced seismicity, Lucky Friday Mine, northern Idaho. *Expl. Min. Geol.* **4,** 65–71.

McGarr, A. (1992). Moment tensors of ten Witwatersrand mine tremors, *Pageoph* **139,** 781–800.

Pechmann, J. C., W. R. Walter, S. J. Nava, W. Arabasz (1995). The February 3, 1995, M_L 5.1 seismic event in the Trona Mining District of Southwestern Wyoming, *Seism. Res. Lett.* **66,** 25–34.

Scott, D. F. (1993). Geologic investigation near an underhand cut-and-fill stope, Lucky Friday Mine, Mullan, Idaho, BuMines Report of Investigations 9470, U.S. Bureau of Mines, Washington, D.C., 25 pp.

Sprenke, K. F., M. C. Stickney, D. A. Dodge, and W. R. Hammond (1991). Seismicity and tectonic stress in the Coeur d' Alene mining district, *Bull. Seism. Soc. Am.* **81,** 1145–1156.

Stickney, M. C., and K. F. Sprenke (1993). Seismic events with implosional focal mechanisms in the Coeur d' Alene mining District, northern Idaho, *J. Geophys. Res.* **98,** 6523–6528.

Stump, B. W., and L. R. Johnson (1977). The determination of source parameters by the linear inversion of seismograms, *Bull. Seism. Soc. Am.* **67,** 1489–1502.

Talebi, S. (1997). Panel discussion, Workshop on Induced Seismology, 18 June 1996, *Pure Appl. Geophy.* **150,** 705–720.

Taylor, S. R. (1994). False alarms and mine seismicity: an example from the Gentry Mountain mining region, Utah, *Bull. Seism. Soc. Am.* **84,** 350–358.

Trifu, C.-I., D. Angus, and V. Shimila (2000). A fast evaluation of the seismic moment tensor for induced seismicity, *Bull. Seism. Soc. Am.* **90,** 1521–1527.

Udias, A. (1999). *Principles of Seismology*, Cambridge University Press, New York, 475 pp.

White, B. G., and J. K. Whyatt (1999a). Differential wall rock movements associated with rock bursts, Lucky Friday Mine, Coeur d'Alene Mining District, Idaho, USA, in *Rock Mechanics for Industry*, B. Amadei, R. L. Kranz, G. A. Scott, and P. H. Smealie (Editors), Balkema, Rotterdam, 1051–1059.

White, B. G., and J. K. Whyatt (1999b). Role of Fault Slip on Mechanisms of Rock Burst Damage, Lucky Friday Mine, Idaho, USA, in *SARES 99: 2nd Southern African Rock Engineering Symposium, Implementing Rock Engineering Knowledge*, T. O. Hagan (Editor), Johannesburg, 13–15 September, 1999, International Society for Rock Mechanics, Johannesburg, 169–178.

Whyatt, J. K., W. Blake, and T. J. Williams (1997). Classification of large seismic events at Lucky Friday Mine, *Trans. Inst. Mining Metall.* **106,** A148–A162.

Whyatt, J. K., T. J. Williams, and W. Blake (1993). Concentrations of rockburst activity and in situ stress at the Lucky Friday Mine, Rockbursts and Seismicity in Mines 1993, R. P. Young (Editor), Balkema, Rotterdam, 135–139.

Geological Sciences
University of Idaho
Moscow, Idaho 83844
(K.F.S.)

Spokane Research Laboratory
315 E. Montgomery
Spokane, Washington 99207-2291
(B.G.W., J.K.W.)

Battelle Memorial Institute
Pacific Northwest Division
Richland, Washington 99352
(A.C.R.)

Earthquake Studies Office
Montana Bureau of Mines and Geology
Butte, Montana 59701
(M.C.S.)

Manuscript received 1 February 2001.